Laser cooling of metastable He atoms in an inhomogeneous electric field

R. Schumann, C. Schubert, and U. Eichmann
Max-Born-Institut for Nonlinear Optics and Short Pulse Spectroscopy, D-12489 Berlin, Germany

R. Jung and G. von Oppen
Technical University Berlin, D-10268 Berlin, Germany

(Received 1 October 1998)

We have investigated laser cooling of metastable helium atoms by laser light at 389 nm using inhomogeneous electric fields for compensating the varying Doppler shift. As a result of the high polarizability of the upper cooling level, we were able to compensate for the large Doppler shift associated with the UV transition frequency and the high beam velocity with moderate field strengths. The method represents an alternate way to the standard Zeeman slowing technique. It is expected to be superior in applications, where high magnetic fields cannot be tolerated. [S1050-2947(99)03703-8]

PACS number(s): 32.80.Rm, 31.50.+w, 32.30.Jc

I. INTRODUCTION

The technique of laser cooling and decelerating an atomic beam is well matured by now and has been applied successfully to a variety of atoms [1]. In particular the so-called *Zeeman slower* has been established as a standard technique to slow atomic beams very efficiently [2,3]. Alternate slowing techniques have been investigated in recent years [4–8], among which the technique of slowing atoms in inhomogeneous electric fields has been successfully demonstrated [9,10]. The latter investigations were partly driven by the fact that laser cooling in inhomogeneous electric fields proceeds similarly as in magnetic fields, but has the advantage that electric fields can be almost perfectly shielded. However, the Stark shifts of the participating levels in the cooling scheme used in those experiments were rather small. For laser cooling a beam of Na atoms a high electric field strength of more than 200 kV/cm was necessary to compensate for the initial Doppler shift and to hold the atoms in resonance during the cooling process [9]. Thus the cooling method is technically not easy to realize and does not qualify as an equivalent technique to the Zeeman slowing technique. This situation changes, however, if one considers that the polarizability respectively the Stark shift scales with the principal quantum number n as n^7. Consequently, using a higher excited level in the cooling scheme results in largely reduced electric fields. We note that the level shift in magnetic fields exploited in the *Zeeman slower* is independent of the principal quantum number n and does not allow easily for a compensation of large Doppler shifts. Advantageous is the fact that the larger photon energy necessary to drive the cooling transition gives rise to a higher momentum transfer to the atom. It leads to a stronger deceleration and consequently to a shorter stopping distance. The larger Doppler shift $\Delta\nu_{\mathrm{Doppler}}=v/\lambda$ associated with the shorter wavelength can be compensated by the Stark shift. We note that a possible large Stark shift is also a prerequisite for laser cooling fast atomic beams such as metastable helium atoms emerging from a discharge source, which have a mean velocity around 2300 m/s.

In this paper we propose and demonstrate efficient laser cooling of an intense beam of He atoms in inhomogeneous electric fields using the above-mentioned ideas. We exploit a new cooling transition at a wavelength of 389 nm, including an upper level with a high polarizability. It enables us to use standard laboratory equipment to provide the voltages. The obtained beam intensity of slow metastable He atoms should be high enough to result in an efficient loading of a neutral particle trap for further experiments such as the investigation of collective effects of a dense sample of these fundamental three-body Coulomb systems. In the case of helium the *Stark slower* represents an alternate method to the Zeeman slowing technique recently applied to cool an intense beam of helium atoms produced in a discharge source [11,12].

II. COOLING SCHEME

Laser cooling in electric fields proceeds in a similar way as laser cooling in magnetic fields [2]. The cooling laser is counterpropagating an atomic beam inside an electric field, whose field strength is increasing along the beam axis. The frequency ν of an atomic transition in an external electric field F_z is given by $\nu=\nu_0+\Delta\nu_{\mathrm{Stark}}$, where ν_0 is the zero-field transition frequency. The Stark shift $\Delta\nu_{\mathrm{Stark}}=-\frac{1}{2}\alpha_{\mathrm{eff}}F_z^2$ depends on the field strength and the effective polarizability α_{eff}, which is determined by the polarizabilities of the initial and final states $\alpha_{\mathrm{eff}}=\alpha_{\mathrm{final}}-\alpha_{\mathrm{initial}}$. Taking into account the influence of the Doppler shift $\Delta\nu_{\mathrm{Doppler}}$ of the laser frequency ν_{laser} seen by the atoms with a velocity v and the Stark shift $\Delta\nu_{\mathrm{Stark}}$ in the electric field, the condition for compensating the decreasing Doppler shift during the cooling process (thus keeping the atoms in resonance with the light of the cooling laser) reads $\nu_0+\Delta\nu_{\mathrm{Stark}}=\nu_{\mathrm{laser}}+\Delta\nu_{\mathrm{Doppler}}$. Assuming a constant deceleration a of the atoms which is based on an average scattering force one obtains a formula for the electric field $F_z(x)$ as a function of the position x of the atoms:

$$F_z(x)=\sqrt{-\frac{2}{\alpha_{\mathrm{eff}}}\left(\Delta\nu_{\mathrm{laser}}+\frac{\nu_{\mathrm{laser}}}{c}\sqrt{v_0^2+2ax}\right)}. \qquad (1)$$

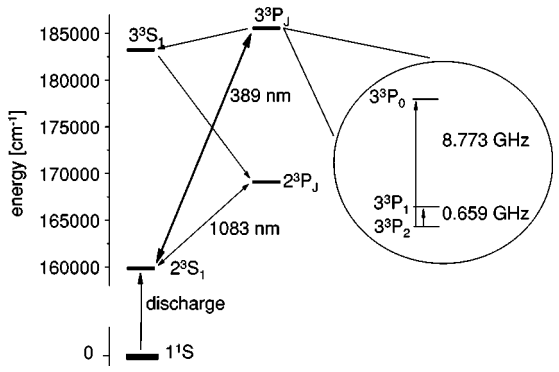

FIG. 1. Level scheme of the helium atom. For more details see text.

Here, v_0 is the initial velocity of the atoms at which the laser deceleration starts and $\Delta\nu_{\text{laser}}$ is the detuning of the laser frequency from the zero-field transition frequency. This field can be realized by using properly matched field plates or, as will be shown, by approximating the exact field through a few segments with linear field plates supplied with appropriate voltages.

To present the cooling scheme we start by showing in Fig. 1 the relevant zero-field level structure of the He atom. The cooling transition involves the metastable $2\,^3S_1$ and the $3\,^3P_2$ levels, which can be driven with a laser wavelength at 389 nm. The $3\,^3P_2$ level has a natural line width of about 1.5 MHz corresponding to a scattering rate of 10^7/s. This is comparable to the scattering rate of the $2\,^3P_2$ state usually exploited in a *Zeeman slower*. The averaged scattering force on the transition $2\,^3S_1 \rightarrow 3\,^3P_2$ is, however, about a factor of 3 larger due to the higher momentum transfer. The fluorescence decay of the upper $3\,^3P_2$ level occurs either directly to the ground state or with a 10% probability via the cascade $3\,^3P_2 \rightarrow 3\,^3S_1 \rightarrow 2\,^3P_J \rightarrow 2\,^3S_1$. The total decay time for the cascade process is only slightly longer than for the direct path, $\tau(3\,^3S) = 36$ ns and $\tau(2\,^3P) = 95$ ns. Additionally, we indicate in Fig. 1 the transition $2\,^3S_1 \rightarrow 2\,^3P_2$ at 1083 nm, which serves in our experiments for the transverse cooling of the beam.

In Fig. 2 we show the $3\,^3P$ level shift in electric fields. A field strength on the order of 35 kV/cm is required to compensate for the initial Doppler shift of roughly 2.5 GHz for the atomic beam with a mean velocity of 1000 m/s. The dominant contribution to the Stark shift comes from the scalar polarizability $\alpha_{\text{scalar}}(3\,^3P) = 4.279$ MHz/(kV/cm)^2, which shifts the center of the energy level, Fig. 2(a) [13,14]. The tensor polarizability, which is almost a factor of 50 smaller than the scalar one $[\alpha_{\text{tensor}}(3\,^3P) = 0.084$ MHz/(kV/cm)^2] gives rise to an $|m|$-dependent Stark shift and thus to a removal of the degeneracy of the magnetic substates with different $|m|$ belonging to a fixed J. This has consequences for the proposed cooling scheme as will be explained later on. In Fig. 2(b) the shift and splitting of the $3\,^3P_2$ magnetic sublevels due to the tensor polarizability are shown. Already at an electric field strength on the order of 30 kV/cm the splitting of different $|m|$ substates exceeds the level linewidth by an order of magnitude.

More specifically, the cooling transition is the $2\,^3S_1(|m| = 1) \rightarrow 3\,^3P_2(|m| = 2)$ transition. This would represent a

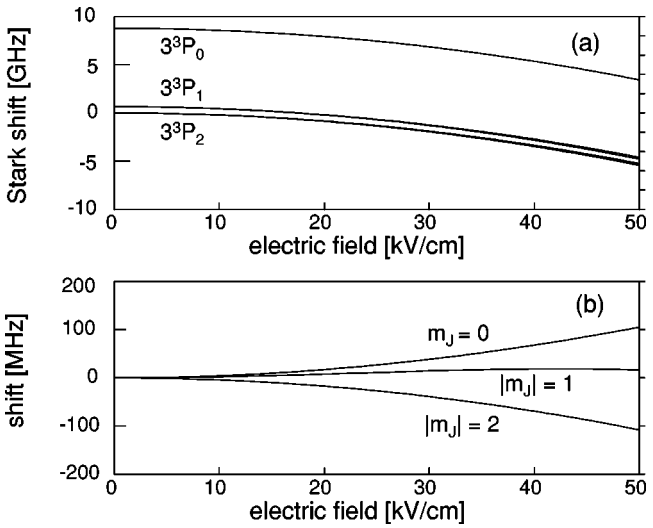

FIG. 2. (a) Stark shift of the ^3P_J mainfold of helium. (b) Stark splitting of the $^3P_2$ due to the tensor polarizability.

closed two-level system in the absence of the cascade decay of the upper level mentioned above. The cascade decay, however, allows for population of the $2\,^3S_1$ $m=0$ ground state. This level is no longer coupled to the upper cooling level because of the selection rules for dipole excitation and, hence, optical pumping may occur. At low electric field strength, where the separation of the magnetic substates is small, optical pumping imposes no problem. Owing to the power-broadened linewidth of the different *m*-substates reexcitation of the $2\,^3S_1$ $m=0$ state to the $3\,^3P_2$ $|m|=1$ state is possible and therefore a repumping back into the cooling scheme. However, at higher electric field strength the separation of the magnetic substates exceeds by far the power-broadened linewidth of the levels and optical pumping occurs. After about 30 absorption-emission cycles all atoms are pumped into the $2\,^3S_1$ $m=0$ state. Consequently the laser cooling process is no longer sustained.

To overcome the problem of optical pumping we exploit the fact that the $2\,^3S_1$ level remains almost degenerate in electric fields. Though the $2\,^3S_1$ level is shifted to lower energy by about 100 MHz by an electric field of 50 kV/cm according to its scalar polarizability $\alpha_{\text{sc}}(2\,^3S) = 0.076$ MHz/(kV/cm)^2, the splitting is negligible, because the tensor polarizability $\alpha_{\text{ten}}(2\,^3S_1) = 0.85$ Hz/(kV/cm)^2 is extremely small [15]. Therefore, the $m=0^-$ and 1^- Stark substates, where we used the labeling as in [13], can be mixed by a weak magnetic field B_x on the order of a few gauss perpendicular to the electric field. As a result of this mixing, all three substates of the $2\,^3S_1$ level can be excited to the $3\,^3P_2$ $|m|=2$ states by irradiating the resonance line linearly polarized in the *y* direction perpendicular to the electric field.

III. EXPERIMENTAL SETUP

Figure 3 gives a sketch of our experimental apparatus. The beam of metastable helium is produced by electron impact in a gas discharge burning in the jet expansion between a needle inside a nozzle as cathode and the grounded skimmer as anode. A negative high voltage is applied to the

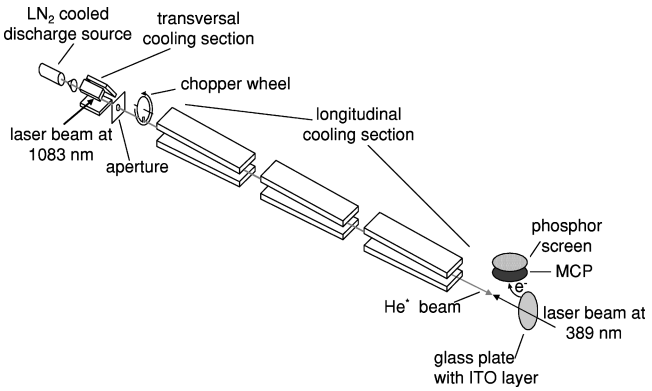

FIG. 3. Sketch of the apparatus. For more details see text.

needle via a 75 kΩ resistor. The nozzle is made of boron nitride, which combines the property of electric isolation with good thermal conductivity and which is easily machinable. The opening of the nozzle to the vacuum side of the source chamber has a 0.2 mm diameter and a length of about 2 mm. To reduce the initial beam velocity of 2300 m/s down to 1100 m/s the tip of the nozzle is mounted onto a copper ring, which is at liquid nitrogen temperature. The skimmer is a conical aperture with a 1 mm diameter, which is placed about 5 mm in front of the nozzle. Furthermore, it separates the source chamber from the cooling chamber. The cooled helium source produces 1.2×10^{14} metastable atoms s^{-1} sr^{-1} running at a current of 2.0 mA. This value has been determined by measuring the beam intensity with a Faraday cup assuming a detection efficiency of 70%. The source chamber is pumped by a 500-l/s turbomolecular pump, resulting in a background pressure of about 1.5×10^{-4} mbar with the discharge on. About 8 cm from the skimmer is a three-mirror construction which allows for transversal cooling [16] . The laser beam from a diode laser at 1083 nm crosses the atomic beam 3 times from directions separated by 120°, thus achieving transversal Doppler cooling. The diode laser (SDL-6702-H1) is a free-running diode which is temperature and current stabilized. The laser beam of about 30 mW is shaped by two cylindrical lenses to a width of about 5 cm and a height of about 1 cm.

After the transverse cooling section the atomic beam is further collimated by an aperture with a 3 mm diameter to avoid collisions of the intense metastable beam with the field plates, which might result in HV discharges between the electric field plates. The atomic beam is mechanically chopped, when it enters the longitudinal laser cooling section. This makes possible time-of-flight measurements to determine the final velocity of the atoms. After the longitudinal cooling section of about 2 m length the atoms hit a grounded glass plate covered by a thin indium-tin oxide (ITO) layer, which is electrically conducting and sufficiently transparent for the cooling laser light. Through the high excitation energy of metastable helium atoms, electrons are emitted from the ITO layer, which are detected by a Chevron multichannel plate (MCP) detector. The signal is further amplified and recorded with a digitizing oscilloscope. Alternately, to obtain atomic beam profiles the detector could be replaced by a position-sensitive detector setup consisting of an electron zoom lens for imaging electrons from the ITO layer, a MCP detector with a phosphor screen, and a charge-coupled device (CCD) camera.

The longitudinal cooling section consists of three pairs of field plates, each having a length of 50 cm and a width of 4 cm. The separation of the field plates decreases from typically 1.2 cm at one end down to 0.8 cm at the other end to provide an inhomogeneous field along the axis. By means of fine adjustment screws the slope of the individual segments can be varied, which enables us to find the optimal electric field along the beam axis or to control the final beam velocity. Perpendicular to the atomic beam the electric field is nearly homogeneous. Voltages up to 25 kV can be supplied separately to one field plate of each segment. Outside the vacuum the whole longitudinal cooling section is surrounded by a coil producing a small magnetic field of about 0.1 mT parallel or antiparallel to the direction of the atomic beam and transversal to the electric field.

The longitudinal cooling laser at 389 nm enters the vacuum chamber through a glass window. After passing the ITO-covered glass plate of the detector it interacts with the counterpropagating atomic beam. The cooling laser beam is linearly polarized and shaped by two lenses to optimize the overlap with the atomic beam. The UV light is produced by external cavity frequency doubling of a commercial cw-Ti:sapphire laser using a LBO crystal. We obtain routinely more than 120 mW of UV light from about 1.5 W of light at 778 nm.

IV. EXPERIMENTAL RESULTS AND DISCUSSION

In order to enhance the atomic beam intensity we collimate the beam by means of a laser diode at 1083 nm. Measurements were performed with the position-sensitive detector to obtain information on the beam profile. We mention that the UV light stemming from the discharge was largely suppressed in these measurements. Figure 4(a) shows the atomic beam profile with no cooling laser. Clearly visible is the spreading of the beam in the *y* direction, while it is limited by the field plates in the *z* direction. Figure 4(b) displays the enhancement of the beam intensity, when we tune the wavelength of the laser diode below resonance. The signal typically increases by a factor of 2–3. In Fig. 4(c) the laser diode wavelength is detuned to the blue side of the resonance. As a consequence, the atomic beam is heated up considerably, leading to a large deflection of atoms, so that they no longer reach the detector.

In order to slow the atomic beam longitudinally we detune the counterpropagating cooling laser 2.3 GHz below the zero-field resonance $2\,^3S_1\rightarrow3\,^3P_2$. With the laser polarization perpendicular to the field axis only $\Delta m=\pm1$ transitions are driven. As already mentioned the slowing of atoms leads to a longer time of flight, which is measured in our experiments. The transformation to absolute velocities is achieved by simulating the laser cooling process as will be presented later. In Fig. 5(a) the time-of-flight distribution of atoms is shown under zero-electric-field conditions but with the cooling laser on. Obvious is the influence of the laser on the distribution indicated by the dip at 2.2 ms. At a laser detuning of 2.3 GHz the transition $2\,^3S_1\rightarrow3\,^3P_2$ of the atoms in the velocity class around 900 m/s is shifted into resonance. In Figs. 5(b)–5(d) we show the influence of voltages applied

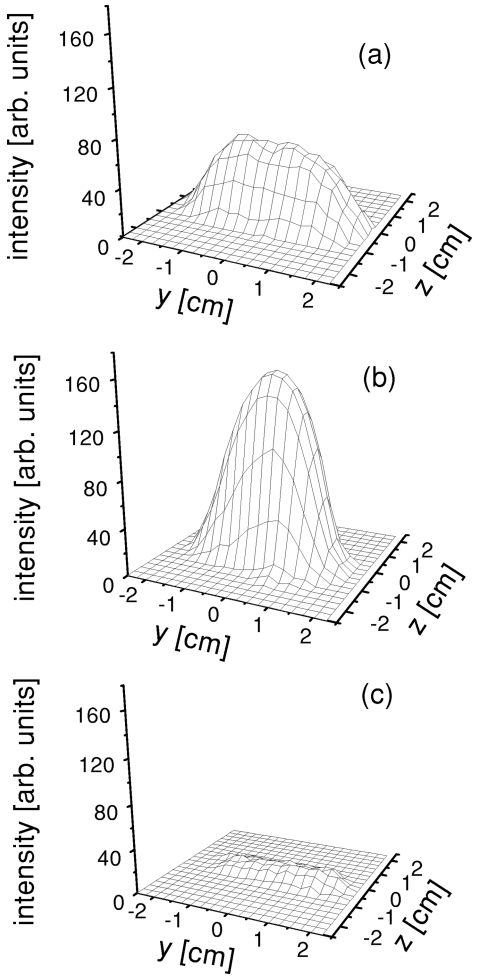

FIG. 4. Transverse beam intensity profiles as a function of the detuning of the transverse cooling laser diode: (a) without the laser, (b) laser slightly detuned to the red of the resonance, and (c) laser slightly detuned to the blue side of the resonance.

consecutively to the three field plate segments. The voltage applied to the first segment is adjusted such that the cooling transition of atoms with a velocity around 850 m/s is in resonance with the laser light. Clearly visible in Fig. 5(b) is the deceleration of a large fraction of atoms to lower velocities, peak *A*. The initial field plate separation of the second segment and the applied voltage are adjusted that the decelerated atoms from the first segment are in resonance. Optimizing the electric field strength along the beam axis in the second segment by fine-tuning the slope of the field plates the atoms are slowed down, further resulting in an increase of the time of flight by more than 0.5 ms as can be seen in Fig. 5(c), peak *B*. It is also visible that not all previously decelerated atoms are further affected by the laser light, so that peak *A* is still visible. This is a result of an improper matching of the field at the end of the first segment and at the beginning of the following segment. Optimizing the voltage and the slope of the third segment enables us to slow down the atoms even further as indicated by peak *C* at around 4.6 ms in Fig. 5(d). The additional structure *D* in Figs. 5(b)–5(d) arises from the interaction with atoms at higher velocities on the transition $2\,^3S_1 \rightarrow 3\,^3P_1$. The origin of the strong decreasing of the peak height as the cooling proceeds stems from transversal heating, which is the dominant loss mechanism for light atoms. It can be compensated by cooling the atoms transversely before they enter the longitudinal cooling setup. Although transverse heating is expected to increase with higher momentum transfer [3], the fraction of atoms found in the lowest velocity class is still about 1.5% of the total detected atoms. This result is comparable to the results obtained in Zeeman slowing, an intense beam of helium at 1083 nm [11]. Thus a sufficient loading rate for a magneto-optical trap can be achieved with our cooling technique.

As mentioned before, a weak magnetic field B_x has to be applied for mixing the $m=0$ and 1^- Stark substates of the

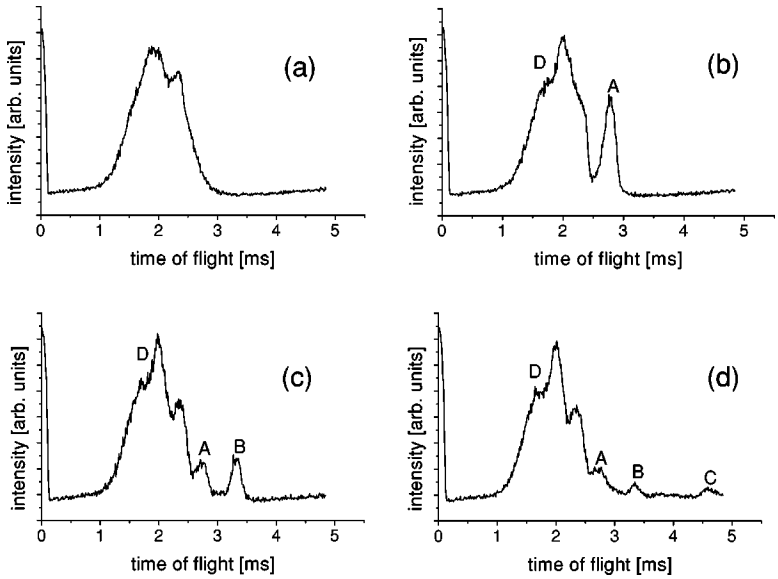

FIG. 5. Time-of-flight distributions for different cooling segments participating in the cooling process. The laser at 389 nm was detuned by 2.3 GHz below resonance. Visible in all spectra is a strong peak at time $t=0$. This stems from the UV light emitted from the discharge source, which is detected by the MCP detector. It serves as a reference point for the time-of-flight distributions. (a) No voltage applied to the cooling segments, (b) 8 kV applied to the first segment, (c) the same, but additionally 20.5 kV applied to the second segment, and (d) the same, but additionally with 22 kV applied to the third segment.

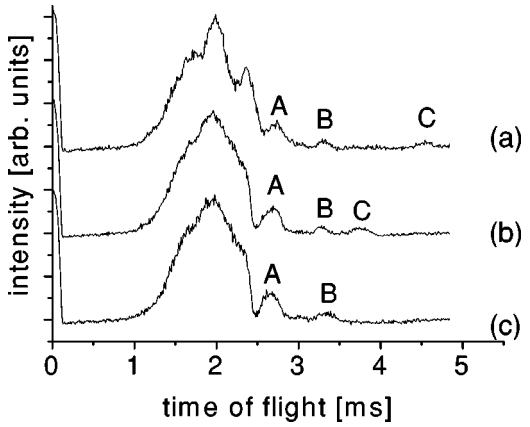

FIG. 6. Influence of an effective magnetic field along the beam axis on the cooling process (a) $B_x = 0.15$ mT, (b) $B_x = 0.012$ mT, and (c) $B_x = 0.003$ mT. Parallel to the electric field axis the Earth's magnetic field is about 0.05 mT.

$2\,^3S_1$ level. In order to investigate the influence of magnetic fields on our cooling process in more detail we measured time-of-flight distributions as a function of the effective magnetic field along the beam axis. We note that in our experiments the Earth's magnetic field was not compensated. As a result the additional magnetic field in the x direction is only able to compensate for the magnetic field along the beam axis. Nevertheless, this is sufficient to demonstrate the influence of the magnetic field on the cooling process.

In Fig. 6 spectra at three different effective magnetic fields are shown. Figure 6(a) shows the time-of-flight distribution obtained with optimized parameters for the laser detuning and for the three field plate segments. A magnetic field of about 0.15 mT is applied along the atomic beam path. The magnetic field causes sufficient mixing of the Zeeman levels of the metastable ground state, while the Zeeman splitting associated with this magnetic field is below 10 MHz and thus within the saturation broadening of the cooling transition. Peak C in Fig. 6(a) at 4.7 ms indicates that the laser cooling is in effect along all three segments. The efficiency of the cooling process decreases significantly in the last cooling segment, when only the Earth's magnetic field is present, Fig. 6(b). The cooling is interrupted by optical pumping processes resulting in a time of flight for peak C around 3.7 ms. If the magnetic field along the beam axis is compensated to zero, no cooling process is sustained in the last electric field segment. The atoms are optically pumped into the $m=0$ metastable ground state level. As a result of the high electric field strength in the third segment, the splitting of the magnetic sublevels of the metastable ground state exceeds the saturation-broadened transition linewidth, inhibiting a repumping of the atoms back to the cooling transition $2\,^3S_1(|m|=1) \rightarrow 3\,^3P_2(|m|=2)$. Consequently, without an additional magnetic field that mixes the metastable ground state Zeeman levels atoms in the $m=0$ substate are lost for the cooling process.

For the interpretation of the experimental time-of-flight spectra we performed a Monte Carlo simulation to obtain the velocity distribution in the atomic beam. Included in the calculation is the interaction of the atomic beam with both cooling lasers, transversal and longitudinal, under consideration of the detailed geometry of our field plate setup. Absorption

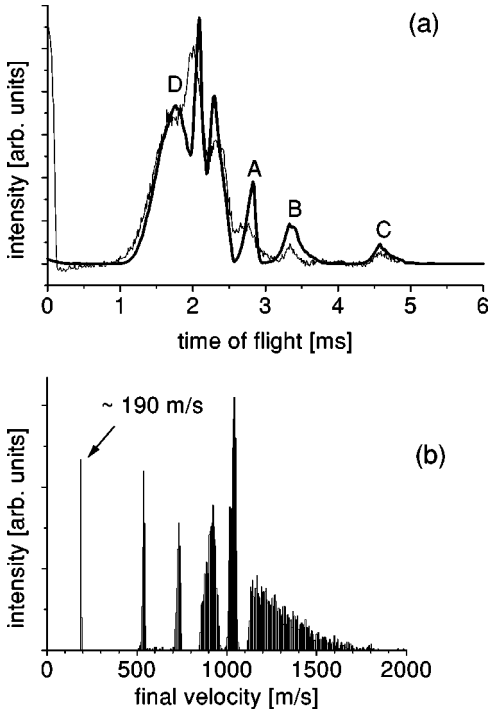

FIG. 7. (a) Comparison of a simulated and an experimental time-of-flight distribution. (b) Velocity distribution in the atomic beam deduced from the simulation shown in (a). About 1.5% of the atoms are decelerated down to 190 m/s.

and emission of a single photon per time step are included in the calculation with a probability that is determined by the laser frequency and its linewidth, the absorption frequency of the atom, which is a function of the position of the atom within the electric field. Furthermore, we take into account the influence of the $3\,^3P_1$ and of the $3\,^3P_2$ levels, which are separated by 658 MHz. However, we do not account for the splitting of the m states due to the tensor polarizability, which is expected to have negligible influence as well as for the cascade decay. The time step in our simulation is given by an exponential decay law with an average life time of the excited states of about 100 ns. Also geometric influences of the overlap between the atomic beam and the laser beam are taken into account. Atoms hitting the field plates during their way through the setup are no longer considered in the calculation. From the calculation, we get information of the fraction of atoms that are laser cooled and their velocity distribution (time-of-flight distribution), which are used to deduce the final velocity from the measured time-of-flight spectra. In Fig. 7(a) we show a comparison of experimental and simulated time-of-flight distributions. The theoretical distributions have been convoluted with a Gauss profile to model the finite opening time of the chopper. Considering the simplicity of the simulation the agreement is more than satisfactory. The peak structure in the experimental time-of-flight distribution is well reproduced. Although the individual peak strengths are not exactly reproduced, the peak positions clearly are. From the result of the calculation we deduce a deceleration of atoms starting from about 850 m/s down to a velocity of 175 m/s. In Fig. 7 (b) we show a velocity distribution determined from the simulation shown in Fig. 7(a). The peak at 4.6 ms in the time-of-flight spectrum corresponds to a velocity of 190 m/s. Thus, the final velocity falls

already in the velocity capture range of standard magneto-optical traps [3]. Nevertheless, a further reduction of the final velocity is desirable. This can be achieved by an optimization of the field plate geometry tailored in such a way that the exact position-dependent field strength according to Eq. (1) is provided. In order to further collimate the beam and reduce particle loss additional transversal cooling sections between the field segments can be implemented.

V. CONCLUSION

In conclusion we report laser deceleration and cooling of a beam of metastable helium atoms in inhomogeneous electric fields. As a result of the high polarizability of the upper level of the cooling transition, only moderate electric fields are necessary to allow for a compensation of the relatively large Doppler shift of about 2.5 GHz and to sustain the laser cooling process. It has been shown that the multilevel structure of the helium atom does not lead to optical pumping, if a small magnetic field is applied along the beam axis. The results show that especially in case of He atoms the *Stark slower* is a convenient method and can be favorably used in cases, where high magnetic fields associated with the *Zeeman slower* cannot be tolerated.

ACKNOWLEDGMENTS

We thank G. Ritter and M. Dammasch for their technical assistance. We thank the Deutsche Forschungsgemeinschaft for financial support.

[1] See, for example, *Laser Manipulation of Atoms and Ions*, Proceedings of the International School of Physics, edited by E. Arimondo, W. D. Phillips, and F. Strumia (North-Holland, Amsterdam, 1992).
[2] W.D. Phillips and H.J. Metcalf, Phys. Rev. Lett. **48**, 596 (1982).
[3] H. Metcalf and P. van der Straten, Phys. Rep. **244**, 203 (1994).
[4] W. Ertmer, R. Blatt, J.L. Hall, and M. Zhu, Phys. Rev. Lett. **54**, 996 (1985).
[5] M. Prentiss and A. Cable, Phys. Rev. Lett. **62**, 1354 (1989).
[6] M. Zhu, W.C. Oates, and J.L. Hall, Phys. Rev. Lett. **67**, 46 (1991).
[7] W. Ketterle, A. Martin, M.A. Joffe, and D.E. Pritchard, Phys. Rev. Lett. **69**, 2483 (1992).
[8] J. Söding, R. Grimm, Yu. B. Ovchinnikov, Ph. Boyer, and Ch. Salomon, Phys. Rev. Lett. **78**, 1420 (1997).
[9] R. Gaggl, L. Windholz, C. Umfer, and C. Neureiter, Phys. Rev. A **49**, 1119 (1994).
[10] J.R. Yeh, B. Hoeling, and R.J. Knize, Phys. Rev. A **52**, 1388 (1995).
[11] W. Rooijakkers, W. Hogervorst, and W. Vassen, Opt. Commun. **135**, 149 (1997).
[12] H.C. Mastwijk, J.W. Thomsen, P. van der Straten, and A. Niehaus, Phys. Rev. Lett. **80**, 5516 (1998).
[13] R. Schumann, M. Dammasch, U. Eichmann, Y. Kriescher, G. Ritter, and G. von Oppen, J. Phys. B **30**, 2581 (1997).
[14] J.P.R. Angel and P.G.H. Sandars, Proc. R. Soc. London, Ser. A **305**, 125 (1968).
[15] M.A. Player and P.G.H. Sandars, Phys. Lett. **30A**, 475 (1969).
[16] U. Drodofsky, J. Stuhler, Th. Schulze, M. Drewsen, B. Brezger, T. Pfau, and J. Mlynek, Appl. Phys. B: Lasers Opt. **65**, 755 (1997).